# The magnetism of rare-earth metals

Although they are chemically similar, these fifteen elements—one sixth of the periodic table—exhibit a broad spectrum of unusual magnetic properties that may be custom controlled by alloying.

Allan R. Mackintosh

In the last two decades a revolutionary improvement has taken place in our understanding of the magnetic behavior of solids. A major contribution to this development has been made with the intense beams of neutrons now available from research reactors. Neutrons interact with magnetic systems through their magnetic moments; the energies, momenta and wavelengths of thermal neutrons correspond with those characteristic of solids. The changes in momentum and energy when a neutron is magnetically scattered in a solid therefore are readily measured,[1] yielding information on magnetic structures and excitations that can not be obtained by other means.

In parallel with this increase in our knowledge of magnetic solids on the microscopic level, an expansion has taken place in the technological applications of magnetic materials. Examples of such applications are improved materials for permanent magnets, magnetic memories and microwave devices. Our theoretical understanding has reached the point at which it is frequently possible to synthesize materials with predetermined magnetic properties, and there is little doubt that the industrial use of such materials in sophisticated devices will continue to increase steadily.

In this article I will review briefly our knowledge and understanding of the magnetism of the largest group of magnetic elements, the rare-earth metals, which comprise about one sixth of all the stable elements. Although less familiar than the transition-metal ferromagnets, iron, cobalt and nickel, the rare earths and their compounds form a class of materials with an enormous variety of magnetic properties. Furthermore, despite this variety, they are in many respects better understood than more familiar magnetic substances. As we shall see, their behavior can be explained qualitatively—and often quantitatively—in terms of two fundamental magnetic interactions that, depending on the circumstances, can give rise to a remarkable variety of phenomena.

The rare-earth metals resemble one another chemically and in many of their physical properties, but they have very different magnetic properties. The reason is that the major part of their chemical and physical behavior is determined by the 5d and 6s valence electrons, while the successive filling of the 4f shell in the rare earth series is responsible for the rich variety of their magnetic properties.[2] Perhaps the most striking manifestation of this variety is the qualitative difference between the magnetic behavior of the light and the heavy rare earth metals, but it may also be observed in substantial differences between the magnetism of neighboring elements, which are otherwise very similar. The fact that the rare earths display the largest known magnetic moments, magnetic anisotropies and magnetoelastic effects makes it possible, by alloying them together, to produce substances with a wide range of magnetic properties.

The chemical similarity between the different rare-earth metals makes their separation a formidable task, and it was not until Frank Spedding and his colleagues at Iowa State University and the Ames Laboratory succeeded in producing pure samples by the ion-exchange method that it was possible to begin acquiring the experimental information necessary for a detailed understanding of their magnetism. Starting in the late 1950's, Spedding, Sam Legvold and their students succeeded in growing pure single crystals and in measuring their basic thermodynamic, magnetic and transport properties. These crystals were made available to Wallace Koehler and his colleagues at the Oak Ridge National Laboratory so that they were able to extend their earlier neutron-diffraction studies, in powder samples, of the magnetic structures. The detailed knowledge of these structures attained in the early 1960's was crucial for the interpretation of the other magnetic properties.

The power of the neutron technique was further demonstrated when Hans Bjerrum Møller and his colleagues at the Risø Research Establishment (Denmark) began their inelastic-scattering investigations of the spin waves in terbium in the middle 1960's. They were able to obtain a rather complete experimental understanding of the magnetic interactions in the heavy rare earths. Figure 1 shows the DR3 reactor at Risø, which is used to provide an intense beam of neutrons for these studies.

In the early 1970's the neutron studies were extended in two important directions:

- At Risø, an extensive series of measurements was initiated on single crystals of the light rare earths, especially praseodymium.
- At Oak Ridge the availability of separated isotopes allowed experiments on many metals that, because of neutron absorption in the natural state, could not be studied by neutron scattering before.

Although in the preceding brief historical survey I have emphasized the role of neutrons in elucidating the magnetic properties of the rare earths, many other measurements (for example, of magnetic susceptibility, magnetostriction, heat capacity, transport properties, electro-

Allan R. Mackintosh is a professor of physics at the H. C. Ørsted Institute of the University of Copenhagen, Denmark.

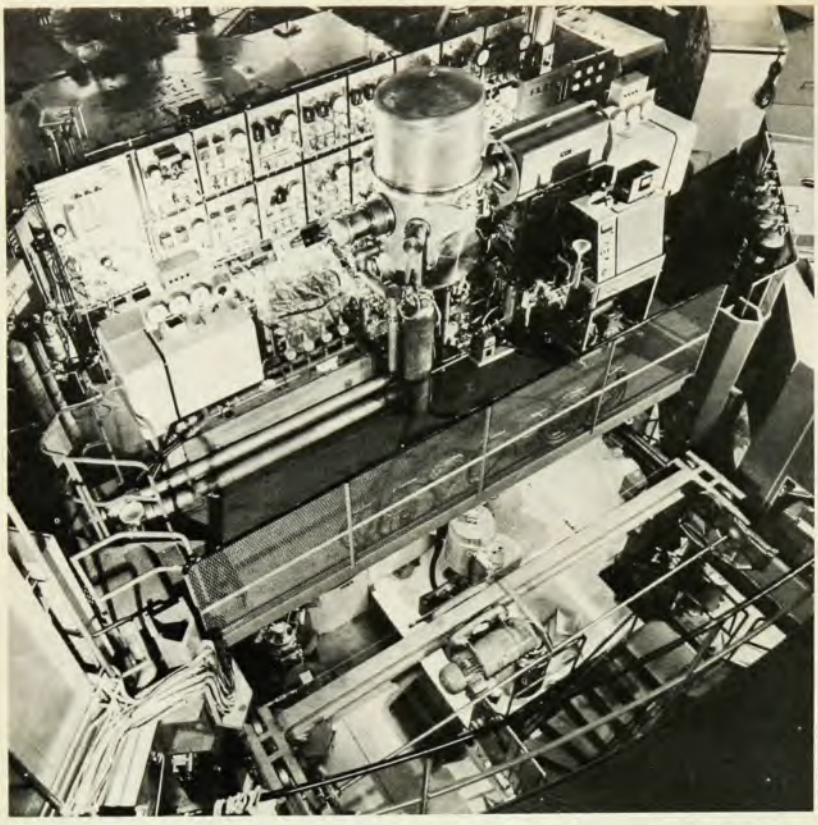

**The interior of the DR3 reactor** at the Risø Research Establishment, Denmark, where much of the data presented in this article was obtained. At the top is the cryogenerator for the cold-neutron source, a container of liquid $H_2$ placed in the reactor to moderate the neutrons, providing an intense beam of long-wavelength neutrons. Crystal spectrometers on the lower level scatter this beam from rare earths to provide information on their magnetic properties. Figure 1

magnetic absorption, nuclear magnetic resonance and the Mössbauer effect) have made valuable contributions. Furthermore, theoretical interpretations and predictions have played a crucial part in suggesting new lines of investigation. Indeed, the development in our understanding of the rare earths over the last twenty years provides an excellent example of the interplay between theory and experiment and of the complementarity of different experimental techniques, both of which are characteristic of modern solid-state physics.

Unlike that of the 3d electrons in the transition metals, the magnetic behavior of the 4f electrons in rare-earth atoms persists when they are assembled in the metallic state. Let us therefore begin with a brief review of the magnetism of the isolated atoms. I will then describe the interactions of rare-earth ions in the metals with their surroundings and with each other, and show how these interactions stabilize the complex magnetic structures of the heavy rare earths. A discussion of the spin-wave excitations from the magnetically ordered state will lead us to consider the way in which these give detailed information about the magnetic interactions. In pointing out the special features of the light rare earths, I shall make particular reference to praseodymium, the one most extensively studied. Finally, a brief survey of some unsolved problems in rare-earth magnetism will give us some indication of trends and perspectives for future research.

### Magnetism in atoms and crystals

The magnetic properties of a rare-earth atom with an incompletely filled 4f shell are determined by *Hund's rules*. These state that, in the ground state, the spin and orbital angular momenta of the individual 4f electrons ($s = \frac{1}{2}$, $l = 3$) combine in such a way that the total spin $S$ is maximized, and, subject to maximum $S$, the total orbital angular momentum $L$ is also maximized. In the first half of the series, the light rare earths, $L$ and $S$ combine in such a way that the total angular momentum is minimized, that is, $J = L - S$; in the heavy rare earths, on the other hand, $J$ is maximized with the value $L + S$. The results of applying these rules through the rare-earth series are given in the table on this page. The magnetic moment in the ground state is given by $g\mu_B J$, where $\mu_B$ is the Bohr magneton and $g$ the Landé factor, also given in the table. Because of the relatively large spin-orbit coupling, only the lowest $J$ multiplet is normally populated at room temperature and below.

When rare-earth atoms condense to form a metal, with a regular structure such as those illustrated in figure 2, the 5d and 6s valence electrons are freed from the atoms and form the conduction electron gas. The 4f electrons lie well within the ion core, however, and are consequently rather effectively shielded from their surroundings by the 5s and 5p electrons. They therefore retain their magnetic properties, as summarized in the table. Nevertheless, they do experience their surroundings through a number of interactions, predominantly the *exchange interactions* and the *crystal-field interactions*.

The exchange interaction between the 4f spin **S** localized at a site **R** and a con-

**Magnetic properties of the rare earths**

| Element (ion) | $L$ | $S$ | $J$ | $g$ | $(g-1)^2J(J+1)$ | $T_c$(K) |
|---|---|---|---|---|---|---|
| Lanthanum ($La^{3+}$) | 0 | 0 | 0 | 0 | 0 | [a] |
| Cerium ($Ce^{3+}$) | 3 | $\frac{1}{2}$ | $\frac{5}{2}$ | $\frac{6}{7}$ | 0.18 | 13 |
| Praseodymium ($Pr^{3+}$) | 5 | 1 | 4 | $\frac{4}{5}$ | 0.80 | [b] |
| Neodymium ($Nd^{3+}$) | 6 | $\frac{3}{2}$ | $\frac{9}{2}$ | $\frac{8}{11}$ | 1.84 | 19 |
| Promethium ($Pm^{3+}$) | 6 | 2 | 4 | $\frac{3}{5}$ | 3.20 | [c] |
| Samarium ($Sm^{3+}$) | 5 | $\frac{5}{2}$ | $\frac{5}{2}$ | $\frac{2}{7}$ | 4.46 | 106 |
| Europium ($Eu^{2+}$) | 0 | $\frac{7}{2}$ | $\frac{7}{2}$ | 2 | 15.75 | 94 |
| Gadolinium ($Gd^{3+}$) | 0 | $\frac{7}{2}$ | $\frac{7}{2}$ | 2 | 15.75 | 293 |
| Terbium ($Tb^{3+}$) | 3 | 3 | 6 | $\frac{3}{2}$ | 10.50 | 230 |
| Dysprosium ($Dy^{3+}$) | 5 | $\frac{5}{2}$ | $\frac{15}{2}$ | $\frac{4}{3}$ | 7.08 | 176 |
| Holmium ($Ho^{3+}$) | 6 | 2 | 8 | $\frac{5}{4}$ | 4.50 | 130 |
| Erbium ($Er^{3+}$) | 6 | $\frac{3}{2}$ | $\frac{15}{2}$ | $\frac{6}{5}$ | 2.55 | 85 |
| Thulium ($Tm^{3+}$) | 5 | 1 | 6 | $\frac{7}{6}$ | 1.17 | 57 |
| Ytterbium ($Yb^{2+}$) | 0 | 0 | 0 | 0 | 0 | [a] |
| Lutetium ($Lu^{3+}$) | 0 | 0 | 0 | 0 | 0 | [a] |

[a] No magnetic moment.
[b] No magnetic ordering above 1 K.
[c] Ordering and critical temperature unknown.

duction electron of spin **s** at position **r** is given by the familiar Heisenberg form $-j(\mathbf{r}-\mathbf{R})\mathbf{S}\cdot\mathbf{s}$. This *s–f exchange interaction* is a straightforward consequence of the Pauli exclusion principle. The antisymmetry of the electronic wavefunction implies an *exchange correlation* for electrons of parallel spin which holds them apart, and hence reduces their Coulomb repulsion energy. When a conduction electron passes in the vicinity of an ion, this interaction results in a force on both it and the localized spin, as illustrated in figure 3. The conduction electron thus carries information on the orientation of the localized spin, which it transmits to other ions by means of the s–f exchange. The net result is an *indirect exchange interaction*[3] between the localized spins which, in a first approximation, also has the Heisenberg form

$$\mathcal{H}_{\rm ff} = -\sum_{\mathbf{R}_{ij}} \mathcal{J}(\mathbf{R}_{ij})\mathbf{S}_i\cdot\mathbf{S}_j \qquad (1)$$

where the *exchange integral* $\mathcal{J}$ is a function of the vector distance $\mathbf{R}_{ij}=\mathbf{R}_i-\mathbf{R}_j$ between the ions. As we shall see, it is the Fourier transform

$$\mathcal{J}(\mathbf{q}) = \sum_{\mathbf{R}_{ij}} \mathcal{J}(\mathbf{R}_{ij})e^{i\mathbf{q}\cdot\mathbf{R}_{ij}} \qquad (2)$$

of this exchange that is most readily measured. This quantity is given in terms of the s–f exchange and the properties of the conduction-electron gas by

$$\mathcal{J}(\mathbf{q}) = (2/N)|j(\mathbf{q})|^2\chi(\mathbf{q}) \qquad (3)$$

The Fourier transform $j(\mathbf{q})$ of $j(\mathbf{r})$ appears squared because of the two interactions involved in the indirect exchange process, and $\chi(\mathbf{q})$ is the Fourier transform of the nonlocal susceptibility of the electron gas, which may in principle be calculated from the electron band structure[4]; $N$ is the number of ions.

The strong spin-orbit coupling in the 4f shell has the effect that **J** rather than **S** is a constant of the motion. The exchange is then determined by the projection of **S** on **J**, which is $(g-1)\mathbf{J}$, so that equation 1 is replaced by

$$\mathcal{H}_{\rm ff} = -\sum_{\mathbf{R}_{ij}} (g-1)^2\mathcal{J}(\mathbf{R}_{ij})\mathbf{J}_i\cdot\mathbf{J}_j$$

$$= -\sum_{\mathbf{R}_{ij}} \mathcal{J}(\mathbf{R}_{ij})\mathbf{J}_i\cdot\mathbf{J}_j \qquad (4)$$

The exchange energy is proportional to $(g-1)^2J(J+1)$ and, as may be seen from the table on page 24, is generally greater in the heavy than in the light rare earths. Characteristic exchange energies in the rare earths correspond to temperatures ranging from tens to hundreds of K.

The magnetic 4f electrons are situated in an inhomogeneous electric field and, because their charge clouds are highly anisotropic, they are subjected to a torque tending to align the moments along particular crystallographic directions, as illustrated in figure 3. This *single-ion magnetic anisotropy* can be very strong,

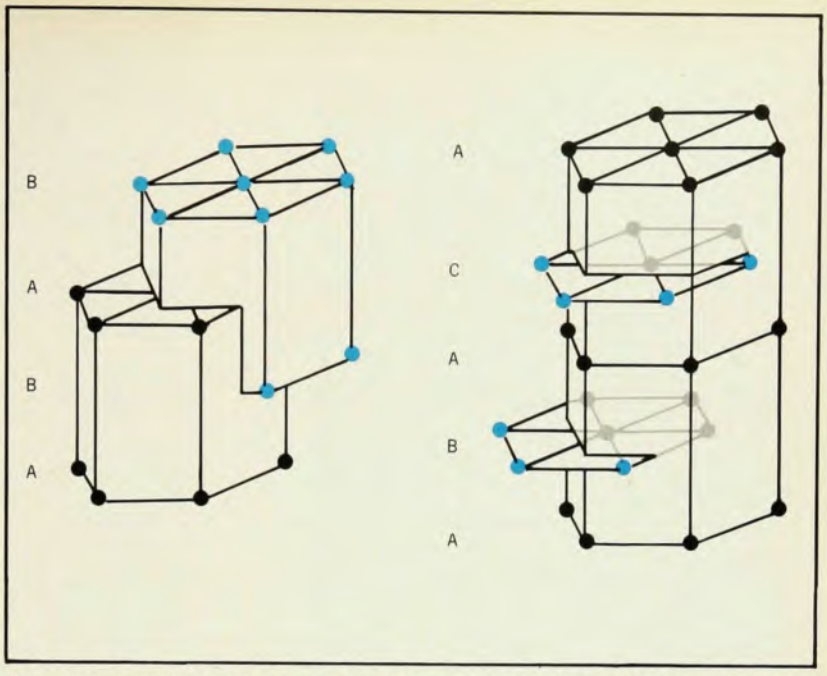


**Two crystal structures of rare-earth metals,** hexagonal close-packed (left) and double hexagonal close-packed (right), differ in their stacking sequences. The hcp structure, the one assumed by all the magnetic heavy rare earths, may be thought of as two interpenetrating simple hexagonal lattices. The **c** axis is coincident with the hexagonal axis, the **a** axis is along a line of atoms in the basal plane and the **b** axis is normal to the other two. The dhcp structure, common among the light rare earths, consists of the sites marked "A," with approximate local cubic symmetry, and equivalent sites, "B" and "C" with hexagonal symmetry. Figure 2

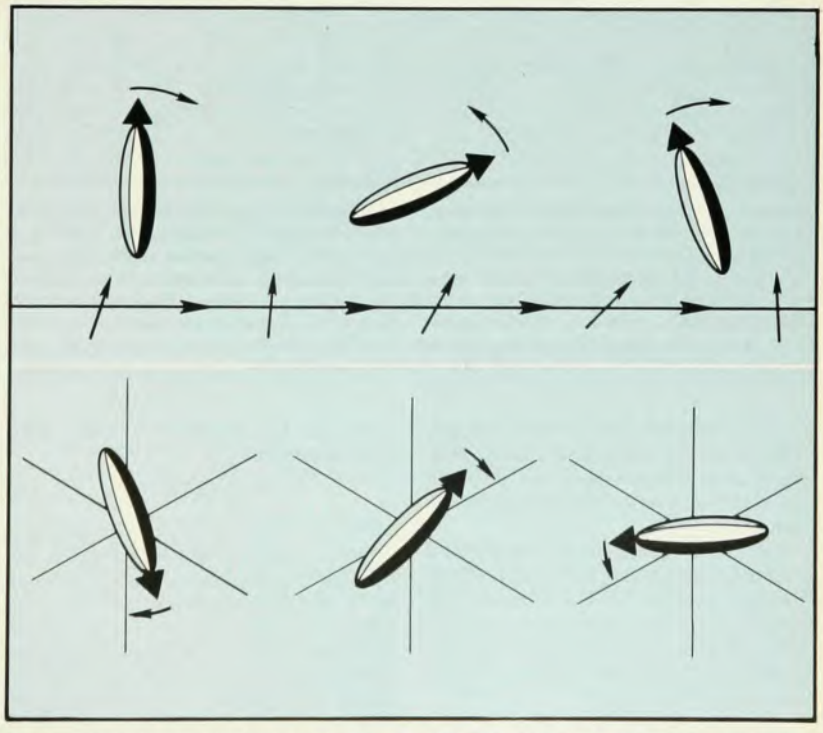

**The two principal magnetic forces** acting on rare-earth ions. In the indirect exchange interaction, above, a conduction electron interacts successively through the s–f exchange with the localized 4f moments, tending to align the latter with particular relative orientations. The result is the effective two-ion exchange interaction. Below, the single-ion crystal-field interaction tends to align the moments along particular equivalent crystallographic directions, but with no preferred orientation relative to each other. In general the two forces act together. Figure 3

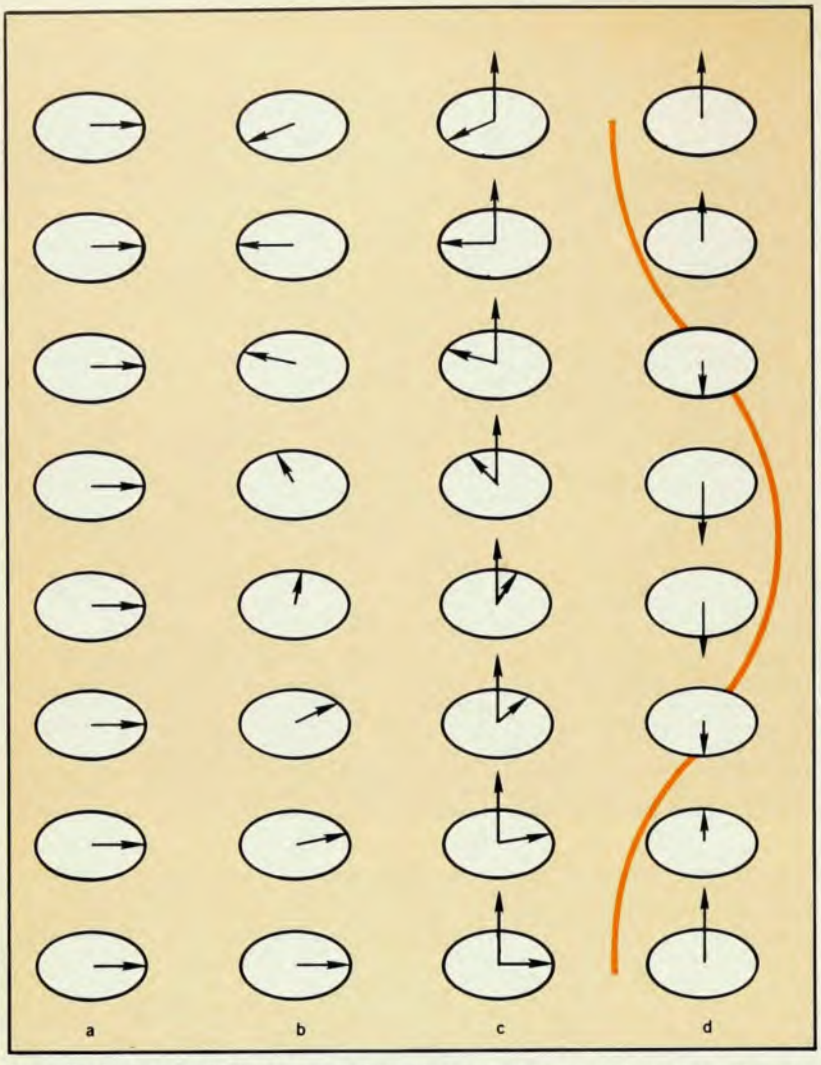


**Magnetic structures of the heavy rare earths.** The moments in a particular hexagonal layer are all parallel. In the *basal-plane ferromagnet*, **a**, all moments are aligned along the direction of magnetization. The moments in the *helix*, **b**, rotate by a specific angle between neighboring planes. The *cone*, **c**, is a combination of a helix and an axial ferromagnetic component, so that the total moment rotates on the surface of a cone. In the *longitudinal wave structure*, **d**, the c-axis component varies sinusoidally, while that in the basal plane is disordered. These structures can all be understood as a combination of the exchange interaction, which produces long-range periodicity along the c axis, and the crystal fields, which tend to orient the moments. Figure 4

requiring magnetic fields of up to millions of gauss to overcome, and making contributions to the energies of the magnetic ions of the same order of magnitude as the exchange energy.

The electrostatic potential experienced by a particular ion may be calculated from Poisson's equation, if it is assumed that the charge that gives rise to this potential lies outside the ion. It may be expanded in spherical harmonics about the center of the ion by the series

$$V(r,\theta,\phi) = \sum_{lm} \gamma_{lm} r^l Y_l{}^m(\theta,\phi) \qquad (5)$$

where the $\gamma_{lm}$ depend on the distribution of the external charge. By applying the general theory of angular momenta, this interaction may be transformed, within a particular LSJ multiplet, to the more convenient form[5]

$$\mathcal{H}_{\rm cf} = \sum_{ilm} B_{lm} O_l{}^m(\mathbf{J}_i) \qquad (6)$$

where $B_{lm} \equiv \alpha_l \gamma_{lm} \langle r^l \rangle$. The so-called Stevens factor $\alpha_l$ for the particular ion includes information about the anisotropy of its charge distribution, while $\langle\ \rangle$ denotes the expectation value for the 4f electrons. The $O_l{}^m(\mathbf{J})$ are the operator equivalents of spherical harmonics, obtained by replacing the Cartesian coordinates in suitably symmetrized spherical harmonics by the Cartesian components of $\mathbf{J}$ so that, for example, $O_2{}^0(\mathbf{J}) \equiv |3J_z{}^2 - J(J+1)|$ and $O_6{}^6(\mathbf{J}) \equiv \frac{1}{2}|(J_x + iJ_y)^6 + (J_x - iJ_y)^6|$. In the hexagonal rare-earth structures, the $z$ axis is usually taken as coincident with the crystal c axis, so that the $x$ and $y$ axes lie in the basal plane.

The great majority of the magnetic properties of the rare earths can be explained in terms of the two contributions to the Hamiltonian for the magnetic ions given by equations 4 and 6.

### Magnetic structures

When cooled below a critical temperature $T_c$, most of the rare-earth metals undergo a transition from a disordered paramagnetic phase to an ordered structure with a regular arrangement of the magnetic moments. These critical temperatures are listed in the table on page 24. The magnetic structures of the heavy rare earths, which may be studied in detail by neutron diffraction,[6] are notable for their long-range periodicity along the hexagonal axis, and the competing strong tendency for the moments to point in particular crystallographic directions. These features may be associated respectively with the special form of the indirect exchange and with the crystal fields. Figure 4 illustrates some of these structures: the basal-plane ferromagnet, the helix, the cone and the longitudinal wave structure.

These forms of ordering may be expressed in terms of two basic structures, the helix and the longitudinal wave. The moments in a particular plane normal to the c axis are aligned in both, but in the *helix* the basal plane components change from plane to plane according to

$$J_{ix} = m\,J\cos\mathbf{Q}\cdot\mathbf{R}_i$$
$$J_{iy} = m\,J\sin\mathbf{Q}\cdot\mathbf{R}_i$$

In the *longitudinal wave* the c-axis component orders in the pattern

$$J_{iz} = m\,J\cos\mathbf{Q}\cdot\mathbf{R}_i$$

Here $\mathbf{Q}$ is the wavevector of the magnetic order and lies along the hexagonal axis; the repeat distance $2\pi/Q$ is many lattice spacings and in general is incommensurable with the lattice periodicity. The relative magnetization $m$ increases monotonically from 0 at $T_c$ to 1 at low temperatures. These structures may occur simultaneously, higher harmonics may be present and $\mathbf{Q}$ may be zero, in which case the magnetization has a ferromagnetic component.

The transition temperature is given in mean-field theory by

$$kT_c = \tfrac{1}{3}\mathcal{J}(\mathbf{Q})(g-1)^2 J(J+1) \qquad (7)$$

A particular metal may form different magnetic structures in different temperature ranges; for example, terbium forms a helical structure between 230 K and 219 K and a ferromagnetic structure at lower temperatures.

The origin of the long-range periodic ordering may be understood by considering the indirect-exchange Hamiltonian of equation 4, which may be written in terms of Fourier transforms as

$$\mathcal{H}_{\rm ff} = -\sum_{\mathbf{q}} \mathcal{J}(\mathbf{q})\mathbf{J}(\mathbf{q})\cdot\mathbf{J}(-\mathbf{q}) \qquad (8)$$

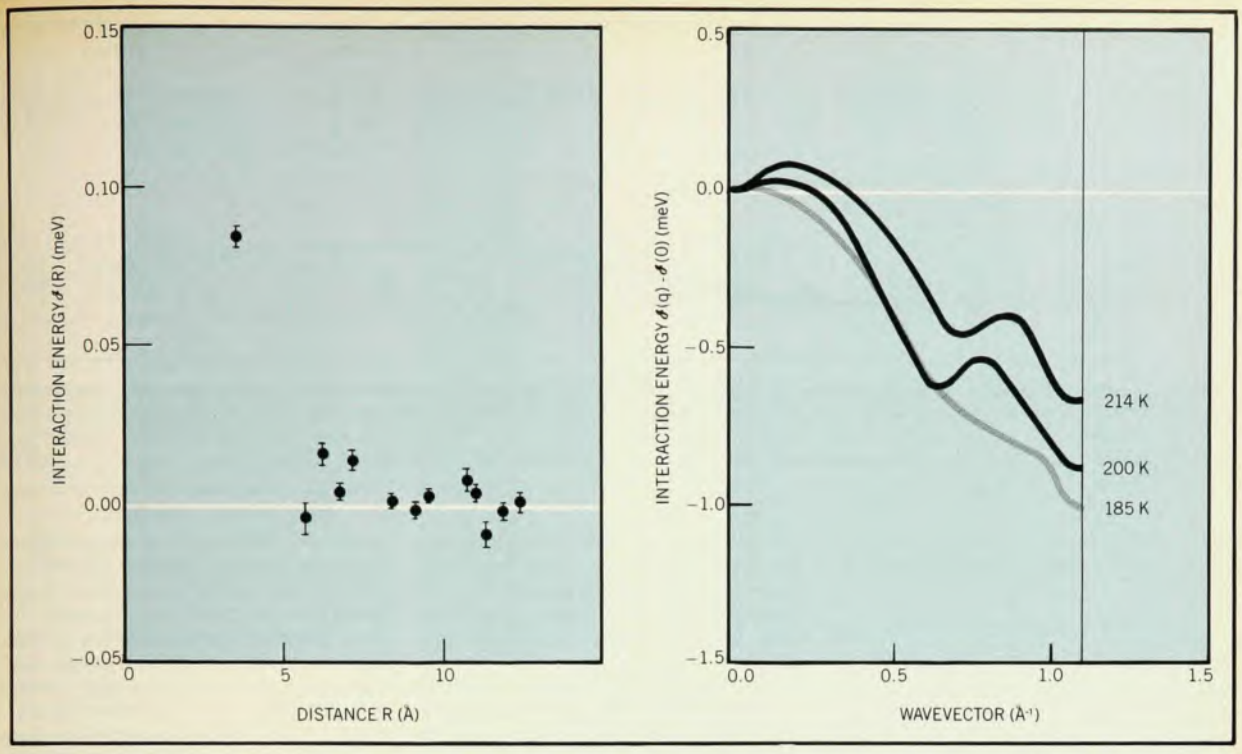


**Exchange in real and reciprocal space** in terbium. Each point in the plot on the left represents the interaction between particular pairs of magnetic ions at 4.2 K; positive values of $\mathcal{J}(\mathbf{R})$ favor a parallel, negative values an antiparallel, alignment. Because it is mediated by the conduction electrons, the exchange interaction is long range and oscillatory. Its Fourier transform (right) in the c direction at 214 K (in an alloy with 10% Ho) exhibits a peak in the helical phase, which stabilizes this phase against the anisotropy forces favoring ferromagnetism. With reduced temperature, this peak becomes less pronounced; it is absent in the ferromagnetic phase at 185 K. Figure 5

where $\mathbf{J}(\mathbf{q}) \equiv N^{-1/2} \Sigma_i \mathbf{J}_i e^{i\mathbf{q}\cdot\mathbf{R}_i}$. Because the sum $\Sigma_\mathbf{q} \mathbf{J}(\mathbf{q})\cdot\mathbf{J}(-\mathbf{q})$ has the constant value $NJ(J+1)$, the contribution of indirect exchange to the total energy will be minimized by the formation of a periodic structure characterized by that value of $\mathbf{Q}$ for which $\mathcal{J}(\mathbf{Q})$ assumes its maximum value.

The indirect exchange in the rare earth metals is mediated by the conduction electrons, and is therefore of long range, as illustrated in figure 5a. Because of the form of the energy bands and Fermi surface,[4] $\chi(\mathbf{q})$ may have a maximum at nonzero $\mathbf{q}$, and hence so may $\mathcal{J}(\mathbf{q})$. An example is shown in figure 5b. Under such circumstances exchange will tend to stabilize a periodic structure.

On the other hand, the crystal fields always tend to align the moments along crystal symmetry directions and hence favor ferromagnetism. For example, if $B_{20}$ in equation 6 is positive, the moments will tend to be in the basal plane, while a negative $B_{20}$ will give a preferred orientation along the hexagonal axis. In terbium and thulium $B_{20}$ is positive and negative respectively, and magnetic fields of several million gauss are required to overcome the axial anisotropy field. Similarly $B_{66}$ gives rise to an anisotropy with hexagonal symmetry, resulting in a preferred orientation within the plane. At low temperatures this hexagonal anisotropy corresponds typically to a field of about 100 kG, which decreases with increasing temperature. All of the structures of figure 4 can be understood in terms of the combination and competition of the indirect-exchange interaction and the single-ion anisotropy fields.

This competition may be illustrated by the transition between the helical and ferromagnetic structures in terbium. Immediately below the Néel temperature, the peak in $\mathcal{J}(\mathbf{q})$ illustrated in figure 5b stabilizes the helical structure. As the temperature is reduced, however, two effects occur that tend to favor the simple ferromagnetic structure:

- The anisotropy forces, which tend to align the moments in the crystallographic b direction, increase, and
- the peak in $\mathcal{J}(\mathbf{q})$ decreases in size, as is also illustrated in figure 5b.

The reason for the latter effect is that the incommensurable magnetic order provides an extra periodicity along the hexagonal axis which, through the s–f exchange, is felt by the conduction electrons. This extra periodicity in the potential gives rise to additional *energy gaps*[7] in the electronic energy spectrum, as periodic potentials always do in solids, and consequently the electron susceptibility $\chi(\mathbf{q})$ and $\mathcal{J}(\mathbf{q})$ are modified. The helical structure therefore tends to destabilize itself as it grows, and eventually the maximum in $\mathcal{J}(\mathbf{q})$ becomes too small to overcome the anisotropy forces, causing a transition to the ferromagnetic structure. Because the electronic structures in the helical and ferromagnetic phases differ somewhat, the peak in $\mathcal{J}(\mathbf{q})$ vanishes below the transition. This need not occur, however; in holmium and dysprosium, for example, the maximum persists through the transition.

### Spin waves

At low temperatures, the magnetic moments in the rare earths are ordered in regular magnetic structures. As the temperature is increased, however, the system of moments becomes progressively disordered. This process can be described in terms of the excitation of *spin waves* in which the moment on each site precesses about the ordered direction with a specified frequency and a corresponding phase relationship to its neighbors, as figure 7 illustrates. The relationship between the frequency and the wavelength, or equivalently between the energy and wavevector of the quantized spin wave, defines the *magnon dispersion relation* $\mathcal{E}(\mathbf{q})$.

When we consider the sinusoidal variation in space and time of the spin wave, we are not surprised that the dispersion relation depends on the Fourier transform, equation 4, of the indirect-exchange

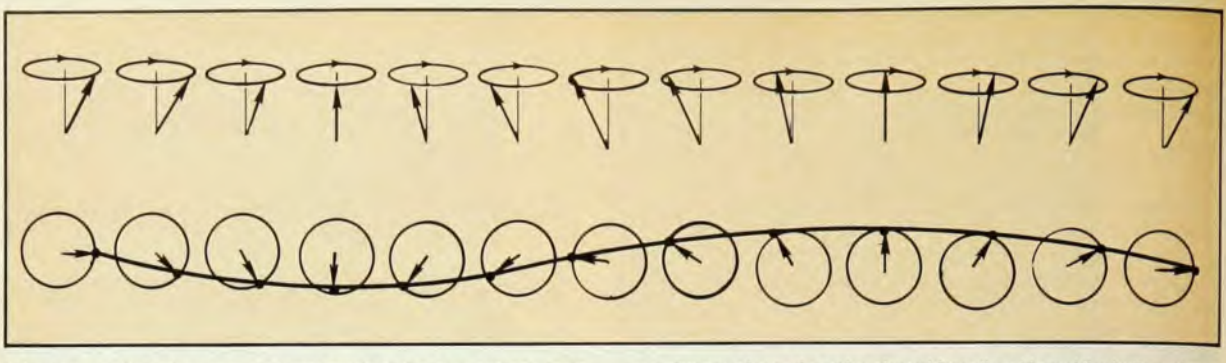

**A ferromagnetic spin wave,** a normal mode of the spin system, is described semiclassically as a precession of each spin about the magnetization direction with a particular frequency. The phase difference between neighboring spins is related to the precession frequency. The top diagram shows the spins viewed from the side and the bottom picture shows the view from above. The energy of such a quantized spin wave, known as a "magnon" (a linear combination of spin deviations), is characterized by a dispersion relation $\mathcal{E}(\mathbf{q})$. Figure 6

interaction. In fact, for an isotropic ferromagnet it is given by the simple expression

$$\mathcal{E}(\mathbf{q}) = J[\mathcal{J}(0) - \mathcal{J}(\mathbf{q})] \qquad (9)$$

The magnon energies can be measured readily by the inelastic scattering of neutrons. If the scattering cross section is measured as a function of the energy transfer from the neutron to the crystal while the momentum transfer is kept constant at a value $\mathbf{q}$, a peak is observed at the energy $\mathcal{E}(\mathbf{q})$, corresponding to the excitation by the neutron of a magnon of this energy and wavevector in the crystal. The whole dispersion relation may then be determined by repeating such a scan for different values of $\mathbf{q}$. The magnon energies have been measured in gadolinium,[8] in which the 4f charge distribution is spherical and the magnetic anisotropy therefore very small, and the form of $\mathcal{J}(\mathbf{q})$ may be deduced directly from the dispersion relation 9.

If the magnetic anisotropy is significant, the Hamiltonian of equation 4 must be augmented by the crystal-field term 6 and the magnon dispersion relation becomes more complicated. In terbium, for example, all crystal-field terms except $B_{20}$ and $B_{66}$ may be neglected and the magnon energies in the ferromagnetic phase are given to a good approximation by

$$\mathcal{E}^2(\mathbf{q}) = |J[\mathcal{J}(0) - \mathcal{J}(\mathbf{q})] + 6\,B_{20}J| \times |J[\mathcal{J}(0) - \mathcal{J}(\mathbf{q})] + 36\,B_{66}J_5| \qquad (10)$$

where $J_5 \equiv (J - \frac{1}{2})(J - 1) \ldots (J - \frac{5}{2})$. Again the dispersion gives $\mathcal{J}(\mathbf{q})$ in a rather direct way but, in contrast to the isotropic ferromagnet, the magnon energy at zero wavevector in the anisotropic ferromagnet has the finite value

$$\mathcal{E}^2(0) = 216\,B_{20}B_{66}JJ_5 \qquad (11)$$

The origin of this *magnon energy gap* is easily understood. For long-wavelength spin waves, the deviations between neighboring moments tend to zero and hence so does the contribution of the exchange to the excitation energy, but it still requires energy to turn the spins against the anisotropy fields. As a result, the magnon energy can not be less than that in equation 11, the geometric mean of the axial and hexagonal anisotropy energies.

The experimental dispersion relation for terbium,[9] shown in figure 7, immediately illustrates the domination of the exchange energy over the anisotropy energy, characteristic of the heavy rare earths. Such a magnon dispersion relation contains a great deal of information. From equation 10 we may extract $\mathcal{J}(\mathbf{q}) - \mathcal{J}(0)$ and, provided that measurements have been made throughout the Brillouin zone, perform a Fourier transform to give $\mathcal{J}(\mathbf{R})$ in a real space, as in figure 5a.

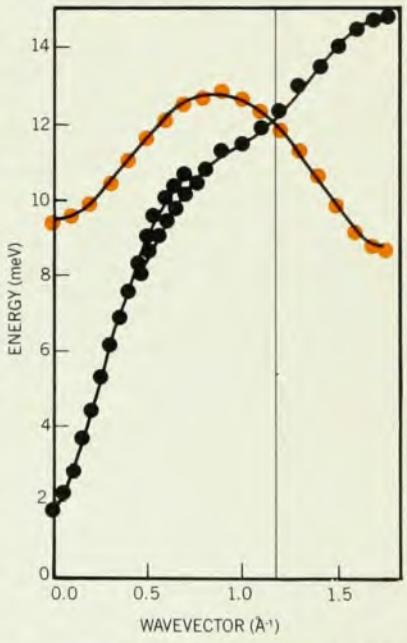


**The energies of magnons** propagating in a direction in terbium at 4.2 K. The dispersion relation has two branches because of the two atoms per unit cell in the hcp structure; the splitting in the lower branch is due to the interaction with the phonons. The exchange forces can be deduced from the dependence of the magnon energy on the wavevector, and the energy gap at zero wavevector gives information about the anisotropy forces. Figure 7

In addition, the dependence on temperature, and more particularly on magnetic field, of the energy gap provides detailed information on the anisotropy fields. Such experiments in terbium have revealed[10] that an important contribution is made to the magnetic anisotropy and magnon energy gap by the interaction between the magnetic moments and the lattice strain, the *magnetoelastic coupling*. Furthermore, the lattice strain has been shown not to follow the precession of the magnetic moments when a spin wave is excited, so that the lattice is effectively *frozen*.

The anisotropy forces acting on a single rare-earth ion therefore comprise the crystalline electric field, the magnetoelastic coupling and the anisotropic exchange, and it is difficult to separate them by means of experiments on pure metals alone. However, the crystal fields can be studied in isolation in dilute solutions of magnetic ions in nonmagnetic hosts. In the free ion, the $2J + 1$ states of different $|M_J\rangle$ are degenerate, but the crystal field in the host metal lifts this degeneracy, and the energy levels and eigenfunctions may be calculated from the Hamiltonian of equation 6. As an example, the eigenstates of terbium in yttrium are shown in figure 8.

By careful measurements and analysis of the magnetization of single crystals over a wide range of temperatures and magnetic fields, supplemented by neutron scattering experiments, Peter Touborg and Jørgen Høg[11] have been able to determine sufficient information about such crystal field levels to allow a reliable deduction of the parameters $B_{lm}$ for a variety of heavy rare-earth ions dissolved in the hexagonal close-packed host metals lutetium, yttrium and scandium. The $\gamma_{lm}$ of equation 5 are found not to depend greatly on either the host or the rare-earth solute, apart from $\gamma_{20}$, which varies in a

systematic way with the ratio $c/a$ of the host's primitive-cell dimensions, so that fairly reliable values may be deduced for the pure magnetic metals from these experiments. It is thereby possible to separate the crystal field, magnetoelastic and exchange contributions to the magnetic anisotropy.

### The light rare earths

As we have noted earlier, the exchange energy, proportional to $(g-1)^2J(J+1)$, is generally smaller in the light than in the heavy rare-earth metals. In addition, the 4f shell is more extended at the beginning of the series so that, according to equation 6, the crystal-field energies are greater. The result is that the dominance of the exchange characteristic of the heavy rare earths is reversed, and the crystal fields tend to dominate in the light rare earths.

The most remarkable manifestation of this situation is found in praseodymium, which has the double hcp structure shown in figure 2. In this structure there are two types of ionic site, which have respectively local hexagonal and (approximately) cubic symmetry. The circumstance that makes the magnetic behavior of praseodymium unique among the elements is that the crystal-field ground states of the ions on both types of site are nondegenerate. According to Kramers's theorem this can only occur for an even number of 4f electrons, because the eigenstates of systems with an odd number of electrons always have even degeneracy. Since a singlet state does not carry a magnetic moment, praseodymium does not display magnetic ordering, even at low temperatures. The magnetic moment is *quenched* by the crystal field.

Of special interest is the behavior on the hexagonal sites, where the lowest $|M_J\rangle$ levels are the singlet $|0\rangle$ and the excited doublet $|\pm1\rangle$, as illustrated in figure 9. The application of a magnetic field can cause a mixing of the excited states into the ground state, giving rise to a magnetic susceptibility per ion $\chi$, which, neglecting exchange, is given at low temperatures by the Van Vleck expression

$$1/\chi = \Delta/2g^2\mu_B{}^2\alpha^2 \qquad (12)$$

where $\alpha \equiv \langle \pm1|J_h|0\rangle$ is the matrix element of the component of $\mathbf{J}$ in the field direction. Since the matrix element of $J_z$ is zero, the application of a moderate field along the c axis produces no moment on the hexagonal sites, as confirmed by neutron diffraction,[12] whereas the susceptibility in the basal plane is quite large. An applied field in the c direction reduces the energy of some of the excited states relative to $|0\rangle$, however, and at 4.2 K a field of 320 kG causes a first-order *metamagnetic* transition to a magnetic phase in which the induced ground state carries a large moment.[13]

If the exchange interaction is included in the molecular field approximation, the reciprocal susceptibility is modified to

$$\frac{1}{\chi} = \frac{1}{g^2\mu_B{}^2}\left[\frac{\Delta}{2\alpha^2} - \mathcal{J}(0)\right] \qquad (13)$$

From this expression, it is apparent that the susceptibility diverges, corresponding to spontaneous ferromagnetism, if

$$2\mathcal{J}(0)\alpha^2/\Delta \geq 1 \qquad (14)$$

The magnetic behavior of such a *singlet ground-state system* is therefore determined by the balance between the exchange and crystal-field interactions. If the exchange is strong enough, magnetic ordering results; otherwise paramagnetism persists down to absolute zero, if the hyperfine interaction with the nucleus is neglected.

The magnetic excitations in praseodymium are quite different from the spin waves discussed earlier. Called *magnetic excitons*, they correspond to linear combinations, with definite phases, of excitations from the ground to excited states on all the hexagonal or cubic ions in the crystal. Despite this difference they may be studied by inelastic neutron scattering in a way that is analogous to the spin-wave measurements described earlier. Such experiments[14] have shown that the isotropic Heisenberg exchange (equation 4) is an oversimplified form for the coupling between the magnetic ions. The results may be interpreted in terms of the *anisotropic interaction*

$$\mathcal{H}_{ff} = -\sum_{\nu,\mathbf{R}_{ij}} \mathcal{J}^{\nu}(\mathbf{R}_{ij}) J_i{}^{\nu} J_j{}^{\nu} \qquad (15)$$

where $\nu$ labels the Cartesian coordinates.

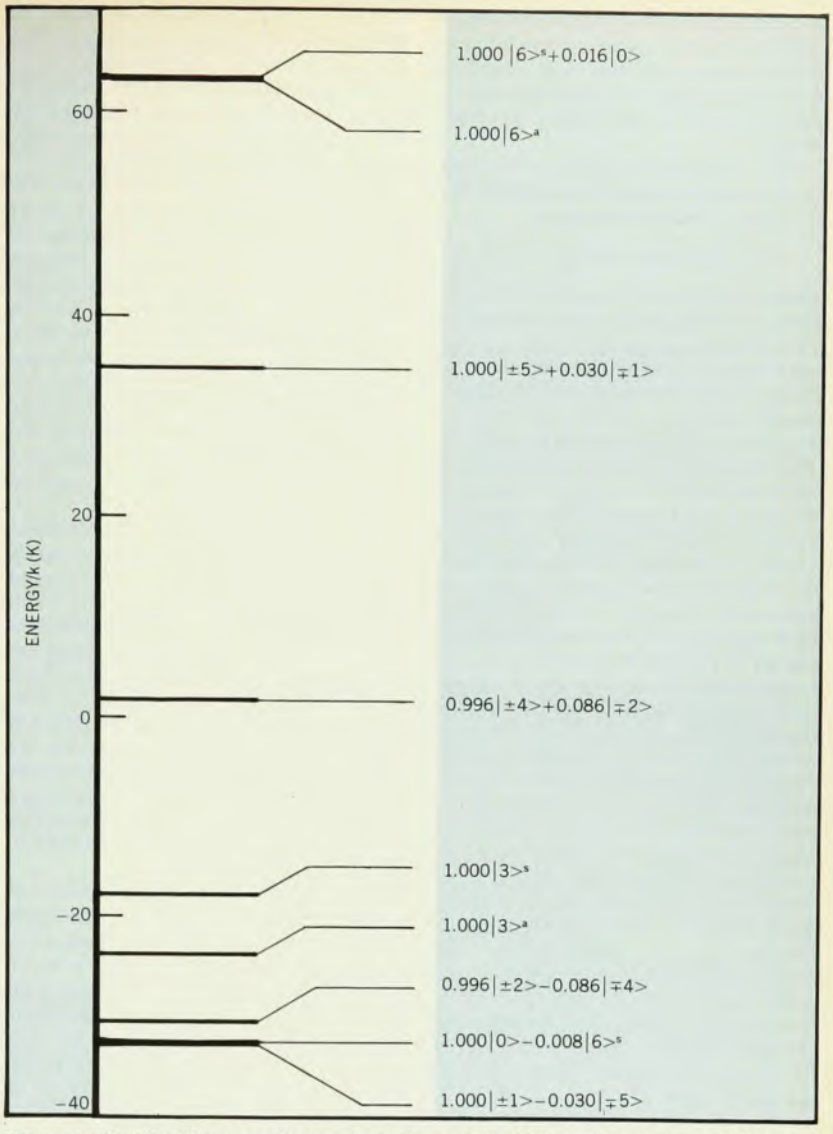


**The energy levels of the magnetic ions** due to the crystal-field interaction may be studied by dissolving a small amount of terbium in nonmagnetic yttrium, so that the exchange interaction is negligible. The $2J+1$ levels corresponding to different values of $M_J$ are degenerate in free space, but the crystal field splits them into the pattern shown. The symbols $|n\rangle^s$ and $|n\rangle^a$ stand for $2^{-1/2}(|n\rangle + |-n\rangle)$ and $2^{-1/2}(|n\rangle - |-n\rangle)$ respectively. Figure 8

Such an expression accounts for the possibility that the exchange energy between parallel moments depends, for example, on whether they are oriented along the hexagonal axis or are lying in the basal plane.

The dispersion relation for the magnetic excitons on the hexagonal sites has the form, at low temperatures,

$$\mathcal{E}^2_{x,y}(\mathbf{q}) = \Delta^2 - 2\alpha^2\,\Delta\mathcal{J}^{x,y}(\mathbf{q}) \quad (16)$$

where $\alpha$ is the matrix element of $J_x$ or $J_y$. In this case the anisotropic exchange lifts the degeneracy of the $|\pm 1\rangle$ states, as figure 9 illustrates. The splitting therefore gives a direct measurement of the exchange anisotropy, which is a substantial proportion of the isotropic component. The dispersion provides a measure of the exchange which, in contrast to that in the heavy rare earths, is small compared with the crystal-field energies.

The steep temperature dependence of the lowest-energy magnetic exciton is illustrated in figure 9. As may be seen from equation 16, the condition for the energy of this mode to go to zero, and hence destabilize the paramagnetic structure, is $2\mathcal{J}^{\nu}(\mathbf{q})\alpha^2/\Delta \geq 1$, which is just a generalization of condition 14 for ferromagnetic ordering. In praseodymium, exchange is about 90% of the value required to drive to zero the energy of this incipient *magnetic soft mode*, which is analogous to the soft phonon modes observed in studies of structural phase transitions.[15] Magnetic ordering has not been observed in neutron-diffraction studies[12] of single crystals, but the addition of a small amount of neodymium results in a periodic magnetic structure, with a $\mathbf{Q}$ and polarization corresponding to this mode. This structure may therefore be considered as a "frozen" exciton.

### Unusual magnets

The detailed understanding of the complex and disparate magnetic properties of the rare-earth metals already attained well illustrates the sophistication of the modern theory of magnetism. Practically all of these properties can be described in terms of the exchange interactions, the crystal fields and the associated magnetoelastic coupling. As we have seen, the relative magnitudes of these interactions give rise to a broad spectrum of magnetic behavior. The heavy rare earths, in which the exchange interaction generally dominates, have been the most thoroughly investigated experimentally; their bulk magnetic properties, magnetic excitations and, at a deeper level of complexity, the interaction of magnons with other excitations,[9] have all been rather thoroughly studied, so that we now have a clear understanding of the relation between the macroscopic and microscopic properties. At the other extreme, in which the crystal fields dominate, the magnetism of praseodymium has recently been elucidated fairly satisfactorily. The intermediate case, in which all interactions have about the same magnitude, is the most difficult to treat, and the study of, for example, samarium, which is further complicated by its complex crystal and magnetic structures, is still only in its early stages.

The phenomenological theory of rare-earth magnetism has reached a level at which it is capable both of explaining the existing data and of predicting new effects. However, the microscopic theory of the magnetic interactions is at a much more rudimentary stage. Some progress has been made in calculating exchange interactions from first principles (although the subtleties of the anisotropic exchange have not yet been included) but computations of the crystal fields and magnetic anisotropy are still almost completely lacking.

Much of the understanding derived from the investigation of the pure metals was subsequently used in explaining and predicting the properties of rare-earth alloys and compounds. The extra freedom derived from placing a rare earth ion in a variable microscopic environment gives rich possibilities—both for producing substances with predictable magnetic properties and for discovering new phenomena. We may expect that this flexibility will be utilized in the future in further improving our understanding of the behavior of rare earth atoms in solids.

Although industrial applications of rare-earth metals have so far been fairly restricted, the increasing sophistication of modern technology could well result in an enhanced demand for metals with unusual, easily variable and precisely defined magnetic properties, a demand the rare earths will be ideally suited to fulfill.

* * *

*I am grateful to many of my fellow rare-earth physicists for interesting and informative discussions of the matters covered in this article, and especially to my colleagues Hans Bjerrum Møller, Jens-Christian Houmann, Jens Jensen, Per-Anker Lindgård and Peter Touborg.*

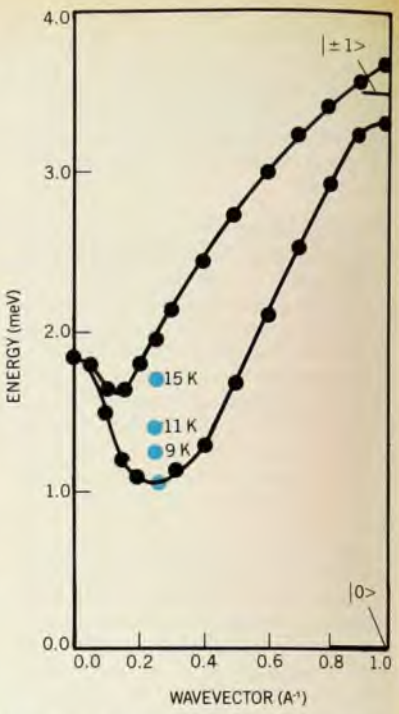


**For magnetic excitations** propagating along the b direction on the hexagonal sites in praseodymium at 6.4 K, exchange produces a dispersion of the transitions between the lowest two crystal-field levels. The anisotropic component splits the $|\pm 1\rangle$ level. As the colored dots show, the energy of the lowest mode depends strongly on temperature. A suitable uniaxial strain could drive the energy of this incipient *soft mode* to zero, giving rise to an antiferromagnetic structure similar to that observed in dilute alloys of Nd in Pr. Figure 9

### References

1. S. H. Chen, S. Yip, PHYSICS TODAY, April 1976, page 32.
2. *Magnetic Properties of Rare Earth Metals* (R. J. Elliott, ed.), Plenum, New York (1972).
3. M. A. Ruderman, C. Kittel, Phys. Rev. **96,** 99 (1954); T. Kasuya, Prog. Theor. Phys. **16,** 45 (1956); K. Yosida, Phys. Rev. **106,** 893 (1957).
4. A. J. Freeman, reference 2, chapter 6; P. A. Lindgård, B. N. Harmon, A. J. Freeman, Phys. Rev. Lett. **35,** 383 (1975).
5. K. W. H. Stevens, Proc. Phys. Soc. **A65,** 209 (1952).
6. W. C. Koehler, reference 2, chapter 3.
7. A. R. Mackintosh, Phys. Rev. Lett. **9,** 90 (1962); H. Miwa, Prog. Theor. Phys. **29,** 477 (1963).
8. W. C. Koehler, H. R. Child, R. M. Nicklow, H. G. Smith, R. M. Moon, J. W. Cable, Phys. Rev. Lett. **24,** 16 (1970).
9. H. Bjerrum Møller, J. G. Houmann, Phys. Rev. Lett. **16,** 737 (1966); A. R. Mackintosh, H. Bjerrum Møller, reference 2, chapter 5.
10. M. Nielsen, H. Bjerrum Møller, P. A. Lindgård, A. R. Mackintosh, Phys. Rev. Lett. **25,** 1451 (1970); J. G. Houmann, J. Jensen, P. Touborg, Phys. Rev. B **12,** 332 (1975).
11. J. Høg, P. Touborg, Phys. Rev. B **14,** 1209 (1976).
12. T. Johansson, B. Lebech, M. Nielsen, H. Bjerrum Møller, A. R. Mackintosh, Phys. Rev. Lett. **25,** 524 (1970); B. Lebech, B. D. Rainford, J. Phys. (Paris) **32,** 370 (1971); B. Lebech, K. A. McEwen, P. A. Lindgård, J. Phys. C. **8,** 1684 (1975).
13. K. A. McEwen, G. J. Cock, L. W. Roeland, A. R. Mackintosh, Phys. Rev. Lett. **30,** 287 (1973).
14. B. D. Rainford, J. G. Houmann, Phys. Rev. Lett. **26,** 1254 (1971); J. G. Houmann, M. Chapellier, A. R. Mackintosh, P. Bak, O. D. McMasters, K. A. Gschneidner Jr, Phys. Rev. Lett. **34,** 587 (1975).
15. J. D. Axe, G. Shirane, PHYSICS TODAY, Sept. 1973, page 32. □